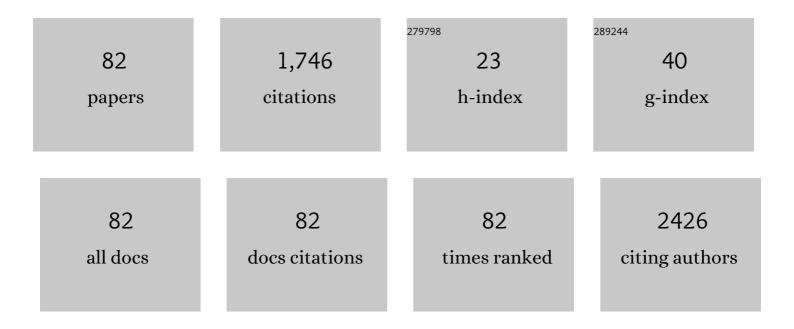
List of Publications by Year in descending order

Source: https://exaly.com/author-pdf/10002673/publications.pdf Version: 2024-02-01



YASUHIRO NINAA

#	Article	IF	CITATIONS
1	Ternary intermetallic LaCoSi as a catalyst for N2 activation. Nature Catalysis, 2018, 1, 178-185.	34.4	221
2	Insights into Initial Kinetic Nucleation of Gold Nanocrystals. Journal of the American Chemical Society, 2010, 132, 7696-7701.	13.7	151
3	Efficient and Stable Ammonia Synthesis by Self-Organized Flat Ru Nanoparticles on Calcium Amide. ACS Catalysis, 2016, 6, 7577-7584.	11.2	129
4	Low-Temperature Synthesis of Perovskite Oxynitride-Hydrides as Ammonia Synthesis Catalysts. Journal of the American Chemical Society, 2019, 141, 20344-20353.	13.7	106
5	Stable single platinum atoms trapped in sub-nanometer cavities in 12CaO·7Al2O3 for chemoselective hydrogenation of nitroarenes. Nature Communications, 2020, 11, 1020.	12.8	94
6	Direct Activation of Cobalt Catalyst by 12CaO·7Al <sub>2</sub> O <sub>3</sub> Electride for Ammonia Synthesis. ACS Catalysis, 2019, 9, 1670-1679.	11.2	68
7	Ruthenium Catalysts Promoted by Lanthanide Oxyhydrides with High Hydrideâ€ion Mobility for Lowâ€Temperature Ammonia Synthesis. Advanced Energy Materials, 2021, 11, 2003723.	19.5	45
8	Ammonia Decomposition over CaNH-Supported Ni Catalysts via an NH <sup>2–</sup> -Vacancy-Mediated Mars–van Krevelen Mechanism. ACS Catalysis, 2021, 11, 11005-11015.	11.2	45
9	High Electron Density on Ru in Intermetallic YRu <sub>2</sub> : The Application to Catalyst for Ammonia Synthesis. Journal of Physical Chemistry C, 2018, 122, 10468-10475.	3.1	43
10	Palladium-bearing intermetallic electride as anÂefficient and stable catalyst for Suzuki cross-coupling reactions. Nature Communications, 2019, 10, 5653.	12.8	43
11	Dynamics of Photoelectrons and Structural Changes of Tungsten Trioxide Observed by Femtosecond Transient XAFS. Angewandte Chemie - International Edition, 2016, 55, 1364-1367.	13.8	42
12	Secreted factors from dental pulp stem cells improve glucose intolerance in streptozotocin-induced diabetic mice by increasing pancreatic β-cell function. BMJ Open Diabetes Research and Care, 2015, 3, e000128.	2.8	39
13	Control of nitrogen activation ability by Co-Mo bimetallic nanoparticle catalysts prepared via sodium naphthalenide-reduction. Journal of Catalysis, 2018, 364, 31-39.	6.2	38
14	Large Oblate Hemispheroidal Ruthenium Particles Supported on Calcium Amide as Efficient Catalysts for Ammonia Decomposition. Chemistry - A European Journal, 2018, 24, 7976-7984.	3.3	34
15	Anchoring Bond between Ru and N Atoms of Ru/Ca <sub>2</sub> NH Catalyst: Crucial for the High Ammonia Synthesis Activity. Journal of Physical Chemistry C, 2017, 121, 20900-20904.	3.1	33
16	Nanoscale in situ observations of crack initiation and propagation in carbon fiber/epoxy composites using synchrotron radiation X-ray computed tomography. Composites Science and Technology, 2020, 197, 108244.	7.8	29
17	Electron Donation Enhanced CO Oxidation over Ru-Loaded 12CaO·7Al <sub>2</sub> O <sub>3</sub> Electride Catalyst. Journal of Physical Chemistry C, 2015, 119, 11725-11731.	3.1	28
18	Amorphous–amorphous transition in a porous coordination polymer. Chemical Communications, 2017, 53, 7060-7063.	4.1	27

#	Article	IF	CITATIONS
19	Nanoscopic origin of cracks in carbon fibre-reinforced plastic composites. Scientific Reports, 2019, 9, 19300.	3.3	27
20	Air-Stable Calcium Cyanamide-Supported Ruthenium Catalyst for Ammonia Synthesis and Decomposition. ACS Applied Energy Materials, 2020, 3, 6573-6582.	5.1	27
21	Direct observation of the electronic states of photoexcited hematite with ultrafast 2p3d X-ray absorption spectroscopy and resonant inelastic X-ray scattering. Physical Chemistry Chemical Physics, 2020, 22, 2685-2692.	2.8	26
22	High-speed x-ray reflectometory in multiwavelength-dispersive mode. Applied Physics Letters, 2008, 92, .	3.3	25
23	Formation and oxidation mechanisms of Pd–Zn nanoparticles on a ZnO supported Pd catalyst studied by in situ time-resolved QXAFS and DXAFS. Physical Chemistry Chemical Physics, 2012, 14, 2152-2158.	2.8	23
24	New high-brilliance beamline BL-15A of the Photon Factory. Journal of Physics: Conference Series, 2013, 425, 072016.	0.4	22
25	In Situ Picosecond XAFS Study of an Excited State of Tungsten Oxide. Chemistry Letters, 2014, 43, 977-979.	1.3	22
26	Effect of hyperglycemia on hepatocellular carcinoma development inÂdiabetes. Biochemical and Biophysical Research Communications, 2015, 463, 344-350.	2.1	19
27	<i>In Situ</i> and Simultaneous Observation of Palladium Redox and Oxygen Storage/Release in Pd/Sr–Fe–O Perovskite Catalysts Using Dispersive XAFS. Materials Transactions, 2013, 54, 246-254.	1.2	18
28	In situ back-side illumination fluorescence XAFS (BI-FXAFS) studies on platinum nanoparticles deposited on a HOPG surface as a model fuel cell: a new approach to the Pt-HOPG electrode/electrolyte interface. Physical Chemistry Chemical Physics, 2014, 16, 13748-13754.	2.8	18
29	Capturing local structure modulations of photoexcited BiVO <sub>4</sub> by ultrafast transient XAFS. Chemical Communications, 2017, 53, 7314-7317.	4.1	18
30	Photoinduced anisotropic distortion as the electron trapping site of tungsten trioxide by ultrafast W L <sub>1</sub> -edge X-ray absorption spectroscopy with full potential multiple scattering calculations. Physical Chemistry Chemical Physics, 2020, 22, 2615-2621.	2.8	15
31	Synergistic Effects of Earth-Abundant Metal–Metal Oxide Enable Reductive Amination of Carbonyls at 50 °C. ACS Applied Materials & Interfaces, 2022, 14, 4144-4154.	8.0	15
32	X-ray-induced reduction of Au ions in an aqueous solution in the presence of support materials andinÂsitutime-resolved XANES measurements. Journal of Synchrotron Radiation, 2014, 21, 1148-1152.	2.4	14
33	Time-Resolved Dispersive XAFS Instrument at NW2A Beamline of PF-AR. AIP Conference Proceedings, 2007, , .	0.4	13
34	Intermetallic ZrPd <sub>3</sub> -Embedded Nanoporous ZrC as an Efficient and Stable Catalyst of the Suzuki Cross-Coupling Reaction. ACS Catalysis, 2020, 10, 14366-14374.	11.2	13
35	Speciation of Tungsten in Natural Ferromanganese Oxides Using Wavelength Dispersive XAFS. Chemistry Letters, 2010, 39, 870-871.	1.3	12
36	Magnetic field-induced spin-crossover transition in [MnIII(taa)] studied by x-ray absorption spectroscopy. Journal of Applied Physics, 2012, 111, 053921.	2.5	12

#	Article	IF	CITATIONS
37	<i>In situ</i> observation of RedOx reactions of Pd/Sr-Fe-O catalysts for automotive emission. Journal of Physics: Conference Series, 2009, 190, 012163.	0.4	11
38	Improvement of a Real Gas-Sensor for the Origin of Methane Selectivity Degradation by µ-XAFS Investigation. Nano-Micro Letters, 2015, 7, 255-260.	27.0	11
39	Time-resolved observation of structural change of copper induced by laser shock using synchrotron radiation with dispersive XAFS. High Pressure Research, 2016, 36, 471-478.	1.2	11
40	Solvation structure of metal ions in nitrogen-donating solvents. Journal of Molecular Liquids, 2006, 129, 18-24.	4.9	10
41	Thermochemical formation of dioxins promoted by chromium chloride: In situ Cr- and Cl-XAFS analysis. Journal of Hazardous Materials, 2020, 388, 122064.	12.4	10
42	Anomaly of the basicity of water in mixed solvents. Journal of Molecular Liquids, 2006, 129, 49-56.	4.9	8
43	Nanoscale in situ observation of damage formation in carbon fiber/epoxy composites under mixed-mode loading using synchrotron radiation X-ray computed tomography. Composites Science and Technology, 2022, 230, 109332.	7.8	8
44	Curved crystal X-ray optics for a new type of high speed, multiwavelength dispersive X-ray reflectometer. Journal of Physics: Conference Series, 2007, 83, 012021.	0.4	7
45	A simultaneous multiwavelength dispersive X-ray reflectometer for time-resolved reflectometry. European Physical Journal: Special Topics, 2009, 167, 113-119.	2.6	7
46	Observation of surface reduction of NiO to Ni by surface-sensitive total reflection X-ray spectroscopy using Kramers–Kronig relations. Japanese Journal of Applied Physics, 2016, 55, 062401.	1.5	6
47	Newly designed double surface bimorph mirror for BL-15A of the photon factory. AIP Conference Proceedings, 2016, , .	0.4	6
48	<i>In situ</i> observation of reduction kinetics and 2D mapping of chemical state for heterogeneous reduction in iron-ore sinters. Journal of Physics: Conference Series, 2016, 712, 012077.	0.4	6
49	High Oxidation Tolerance of Ru Nanoparticles on 12CaO·7Al <sub>2</sub> O <sub>3</sub> Electride. Journal of Physical Chemistry C, 2016, 120, 8711-8716.	3.1	6
50	3D Spectromicroscopic Observation of Yb-Silicate Ceramics Using XAFS-CT. Microscopy and Microanalysis, 2018, 24, 484-485.	0.4	6
51	Femtosecond Charge Density Modulations in Photoexcited CuWO <sub>4</sub> . Journal of Physical Chemistry C, 2021, 125, 7329-7336.	3.1	6
52	A high-temperature in situ cell with a large solid angle for fluorescence X-ray absorption fine structure measurement. Review of Scientific Instruments, 2015, 86, 034102.	1.3	5
53	S100B impairs glycolysis via enhanced poly(ADP-ribosyl)ation of glyceraldehyde-3-phosphate dehydrogenase in rodent muscle cells. American Journal of Physiology - Endocrinology and Metabolism, 2017, 312, E471-E481.	3.5	5
54	Oxidation Number Estimation of Ca in Ca-N Compounds from Ca <i>K</i> -edge XANES Spectra. Bulletin of the Chemical Society of Japan, 2017, 90, 963-965.	3.2	5

#	Article	IF	CITATIONS
55	Nature of the transformation in liquid iodine at 4 GPa. Physical Review B, 2017, 96, .	3.2	5
56	Insulator-to-Metal Transition of Cr2O3 Thin Films via Isovalent Ru3+ Substitution. Chemistry of Materials, 2020, 32, 5272-5279.	6.7	5
57	Conceptual design of the Hybrid Ring with superconducting linac. Journal of Synchrotron Radiation, 2022, 29, 118-124.	2.4	5
58	Kinetic Study of Reduction Reaction for Supported PdO Species by Means of Dispersive XAFS Method. Journal of Physics: Conference Series, 2013, 430, 012053.	0.4	4
59	Development of spectromicroscopes for multiscale observation of heterogeneity in materials at photon factory, IMSS, KEK. AIP Conference Proceedings, 2019, , .	0.4	4
60	Time-Resolved X-Ray Reflectometry in the Multiwavelength Dispersive Geometry. AIP Conference Proceedings, 2010, , .	0.4	3
61	Development of surface sensitive DXAFS measurement method by applying Kramers-Kronig relations to total reflection spectra. Journal of Physics: Conference Series, 2014, 502, 012035.	0.4	3
62	Degradation mechanism of a high-performance real micro gas sensor, as determined by spatially resolved XAFS. Physical Chemistry Chemical Physics, 2016, 18, 7374-7380.	2.8	3
63	Dynamic chemical state conversion of nickel species supported on silica under CO–NO reaction conditions. Catalysis Today, 2018, 303, 33-39.	4.4	3
64	Finding Degradation Trigger Sites of Structural Materials for Airplanes Using Xâ€Ray Microscopy. Chemical Record, 2019, 19, 1462-1468.	5.8	3
65	Development of in situ cell for simultaneous XAFS/XRD measurements at high temperatures. Radiation Physics and Chemistry, 2020, 175, 108153.	2.8	3
66	A surface sensitive hard X-ray spectroscopic method applied to observe the surface layer reduction reaction of Co oxide to Co metal. Physical Chemistry Chemical Physics, 2020, 22, 24974-24977.	2.8	3
67	Time-Resolved Observation of Phase Transformation in Fe–C System during Cooling via X-ray Absorption Spectroscopy. Materials Transactions, 2021, 62, 155-160.	1.2	3
68	Gritty Surface Sample Holder Invented To Obtain Correct X-ray Absorption Fine Structure Spectra for Concentrated Materials by Fluorescence Yield. Analytical Chemistry, 2016, 88, 3455-3458.	6.5	2
69	In situ X-ray absorption fine structure analysis of redox reactions of nickel species with variable particle sizes supported on silica. Journal of Solid State Chemistry, 2018, 258, 264-270.	2.9	2
70	In situ XRM Observation of Cracking in CFRP during Nanomechanical Testing. Microscopy and Microanalysis, 2018, 24, 432-433.	0.4	2
71	In situ TREXS Observation of Surface Reduction Reaction of NiO Film with â^¼2 nm Surface Sensitivity. Chemical Record, 2019, 19, 1457-1461.	5.8	2
72	Dynamics of Photoelectrons and Structural Changes of Tungsten Trioxide Observed by Femtosecond Transient XAFS. Angewandte Chemie, 2016, 128, 1386-1389.	2.0	1

#	Article	IF	CITATIONS
73	Sample exchange robot under an oxygen-free atmosphere for DXAFS experiments. AIP Conference Proceedings, 2019, , .	0.4	1
74	Unique atomic structure of metals at the moment of fracture induced by laser shock. Materials Science & Engineering A: Structural Materials: Properties, Microstructure and Processing, 2022, 831, 142199.	5.6	1
75	Construction and commissioning of direct beam transport line for PF-AR. Journal of Physics: Conference Series, 2017, 874, 012024.	0.4	0
76	In Situ XAFS Observation of Chemical Species Near Solid/Liquid Interface in a Model Reaction of Pitting Process. ECS Transactions, 2017, 77, 831-836.	0.5	0
77	Ultra-Fast XAFS Studies on Photocatalyst Using SACLA. Nihon Kessho Gakkaishi, 2017, 59, 24-28.	0.0	0
78	Development of multi-modal surface research equipment by combining TREXS with IRRAS. AIP Conference Proceedings, 2019, , .	0.4	0
79	Nanoscale crack initiation and propagation in carbon fiber/epoxy composites using synchrotron: 3D image data. Data in Brief, 2020, 31, 105894.	1.0	Ο
80	PF BL-15A for semi-microbeam XAFS/XRF and high-brilliance SAXS/GI-SAXS. Acta Crystallographica Section A: Foundations and Advances, 2014, 70, C1741-C1741.	0.1	0
81	Nano Mechanical Testing for In Situ X-CT Observation of CFRP. , 0, , .		Ο
82	In situ X-CT Observation of Crack Initiation and Propagation in CFRP with X-ray Microscopy. , 0, , .		0